physica status solidi
pss
www.pss-journals.com

reprint

WILEY-VCH

Phys. Status Solidi C **10**, No. 1, 97–100 (2013) / **DOI** 10.1002/pssc.201200551

physica status solidi c
www.pss-c.com
current topics in solid state physics

A quantum dot nucleated on the edge of a threading dislocation: elastic and electric field effects

Grzegorz Jurczak*, **Toby D. Young, and Paweł Dłużewski**

Institute of Fundamental Technological Research of the Polish Academy of Sciences, ul. Pawińskiego 5b, 02-106 Warsaw, Poland

Received 31 July 2012, revised 6 September 2012, accepted 9 October 2012
Published online 7 December 2012

Keywords quantum dot, threading dislocation, piezoelectricity, band edge structure

* Corresponding author: e-mail gjurcz@ippt.pan.pl, Phone: +48-22-8261281 ext.144, Fax: +48-22-8269615

In this work the affect of a threading dislocation localised on the edge of GaN/AlN quantum dot is analysed. A standard piezoelectric continuum model is extended to allow the embodiment of threading dislocations that are modelled as a continuous electro-elastic line defect originating in the matrix material. Two common types of dislocation are considered: an edge-type and a screw-type. It is demonstrated that the presence of a TD provides local region of tensile strain as a preferential condition for GaN QD growth by reduction of the GaN / AlN lattice mismatch. It is found that dislocation induced potential causes a measurable in-plane shift of the electron/hole localisation and an asymmetric decrease in the band-to-band transition energy.

© 2012 WILEY-VCH Verlag GmbH & Co. KGaA, Weinheim

1 Background Type III-nitride semiconductor materials of the wurtzite crystal class are interesting because of their physical properties that lend them as candidates for novel optoelectronic devices [1]. Perhaps the most well investigated example of a III-nitride nanostructure is that of an isolated GaN Quantum Dot (QD) buried in an AlN matrix. Owing to the lattice mismatch between commonly used substrates and nitride layers, defects are introduced into the heterostructure, among others, in the form of Threading Dislocations (TD). The density of TDs in III-nitrides are $\mathcal{O}\,10^9$ to $10^{11}\,\mathrm{cm}^2$ [2,3]. Advances in dislocation-reducing growth techniques can reduce the dislocation density to $\mathcal{O}\,10^7\,\mathrm{cm}^2$; nevertheless, this number is still significantly high.

The impact of dislocations on the optoelectronic properties of QDs is somewhat ambiguous. While the presence of dislocations may facilitate their growth, they also act as non-radiative recombination centres that reduce their optical output, heat-up the device, and reduce their operational lifetime. Remarkably, the density of self-assembled GaN QDs is found to be of the same order of magnitude as the density of dislocations in the AlN matrix [3], and moreover, it is found that QDs recurrently nucleate on the edge of TDs. This strongly suggests a correlation between dislocation arrangement and QD formation. An accepted explanation for this is that the volume of tensile strain originating from the TD reduces the GaN / AlN lattice mismatch and thus composes an energetically favourable site for QD formation.

Experimental techniques developed in electron holography allow the investigator to measure the electrostatic potential present in a defective heterostructure; however, an interpretation of the affect of the dislocation induced potential is tricky because of an apparent discrepancy between reports on the measured potential and its spatial distribution. Measurements between $-0.2\,\mathrm{V}$ and $-3.0\,\mathrm{V}$ for the peak potential with a radial extent of $15\,\mathrm{nm}$ to $50\,\mathrm{nm}$ have been reported for an edge-type dislocation in GaN crystal [4,5]. The corresponding fractional charge density of the dislocation line is between 0.3 and 2.0 electrons per lattice parameter ($^{e}/_{c}$). The peak value of the electrostatic potential related to a screw dislocation reaches $-1.4\,\mathrm{V}$, which corresponds to a fractional charge density of $1.0\,^{e}/_{c}$ [4] with a radial extent reaching $200\,\mathrm{nm}$.

The number of theoretical works that determine the affect of a threading dislocation on a nearby nucleated QD is rather limited; see for example Ref. [6,7]. Furthermore, in both of these references the dislocation line was sup-

© 2012 WILEY-VCH Verlag GmbH & Co. KGaA, Weinheim

posed to be electrically neutral, in contrast to experimental evidence. It is warranted therefore to systematically investigate the electro-mechanical affect of dislocations on the physics of QD structures occupying the matrix.

2 Model In this manuscript, a theoretical investigation of a system composed of a GaN/AlN QD nucleated on the edge of a TD is conveyed using a nonlinear piezoelectric model that is extended to include a charged dislocation line. The theoretical description of piezoelectric materials used here differs from the traditional *linear* piezoelectric problem (as formulated in Ref. [8]). Here a *finite deformation approach* is utilised that is described in detail for defective elastic crystals in Ref. [9]. The description of a TD is facilitated by treating it as an initial plastic deformation according to analytical formulæ describing a displacement field around the dislocation [10]. The singular point at the dislocation core is handled by following the "core-interpolation" prescription given in Ref. [11] with a core radius equal to the length of the Burgers vector. That model is supported here by the electric equation and reciprocal couplings to effectively solve the boundary value problem for a piezoelectric QD heterostructure with a charged dislocation line.

The dimensions of the model of a QD nucleated on the edge of a TD follow from previous experimental observations; see Ref. [3]. The GaN QD base, hat, and height are 17, 4.1, and 3.6 nm respectively, which occupies $10-15\,\%$ of the AlN matrix. A TD is positioned on a corner of the QD's hexagonal base as depicted in Fig. 1. Two distinct and common dislocation types are considered, where each dislocation is described by its own Burgers vector ($\mathbf{b}$). They are:

1. *Edge-type Dislocation* (ED) with a Burgers vector $\mathbf{b} = {}^{1}\!/_{3}\,[\bar{2}110]$ that lies parallel to the x-axis. This orientation is equivalent an additional $(2\bar{1}\bar{1}0)$ half-plane outside of the QD and ending just on the dislocation line.
2. *Screw-type Dislocation* (SD) with a Burgers vector $\mathbf{b} = [0001]$, which is equivalent to a vertical jump in $(2\bar{1}\bar{1}0)$ half-plane equal to one lattice parameter.

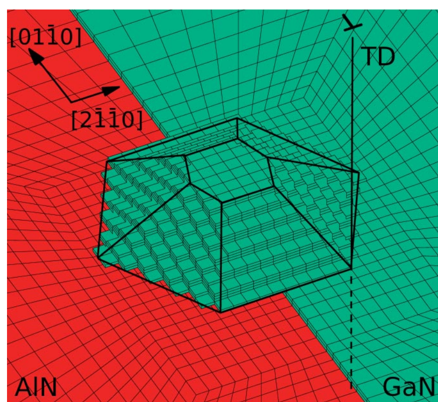

Figure 1 Finite element grid showing the geometry of the quantum dot, a portion of the wetting layer, and the orientation of the threading dislocation line ($\perp$) located on the quantum dot edge. Black lines trace the boundary of the quantum dot.

The dislocation charge density (peak potential) were $1.0\,{}^{e}\!/_{c}$ ($-1.4\,$V) for the SD and $0.3\,{}^{e}\!/_{c}$ ($-0.42\,$V) for the ED, respectively. The fractional charge density of the dislocation, following the experimental observations of Ref. [4], is truncated to a radial extent of 35 nm.

3 Results The results for the two systems sketched above are discussed in this section. Additionally, a *Reference* configuration for comparative discussion in in the main text is considered, that is, an isolated QD in the absence of a TD. Empirical material parameters, i.e. elastic stiffness, piezoelectric coefficients, electric permittivity, and spontaneous polarisation, were taken from Ref. [12].

3.1 Elastic field effects The orientation of the Burgers vector of the ED coincides with the x-axis of a finite element mesh (see Fig. 1) and thus the strain affect is mainly visible in terms of the xx-strain component (upper panel of Fig. 2) and xy-shearing strain (not shown). In the Reference configuration (inset of Fig. 2a) the in-plane (xx- and yy-) strain components peak at around $1.8 - 1.9\,\%$ near the QD facets. The affect of the dislocation is stronger nearer to the dislocation core and even exceeds the Reference strain. This is visible as an area of local tensile strain (rather than compressive strain) on the QD corner. Further, away from the dislocation core, in the center of the QD, the strain is around $1.5\,\%$ which constitutes a $20\,\%$ reduction of the Reference strain value. Around the ED line there are two local strains region of opposite sign (compressive and tensile). In the plane defined by the dislocation line and the Burgers vector, which coincides with the border between compressive and tensile strain fields, there is intensive bending of the crystal lattice. The result is shearing in the xy-plane that reaches $1.4\,\%$.

The Burgers vector of the SD is coaxial with the dislocation line and thus strain effects should be observed for shearing components of the strain defined in planes parallel to the dislocation line. In fact, the SD perturbs mainly xz- and yz-shearing components of strain, see Fig. 2b (*cf.* inset), while leaving the normal components of strain largely unchanged. The vertical jump of the crystal lattice induces an antisymmetric shearing strain state on opposite sides of dislocation line. The peak value of that strain is $\pm 1.0\,\%$, while in the center of QD reduces to around $0.35\,\%$. Similarly as for ED, the affect of the SD is stronger nearer to the dislocation line and also exceeds the Reference strain.

3.2 Electrostatic field effects The potential induced in the system by the presence of a dislocation is axisymmetric around the dislocation line. The affect of this on the electrostatic potential in the $x = [2\bar{1}\bar{1}0]$ and $z = [0001]$ directions through the centre of the QD is given in the upper panel of Fig. 3. There, the electrostatic potential is plot-

© 2012 WILEY-VCH Verlag GmbH & Co. KGaA, Weinheim

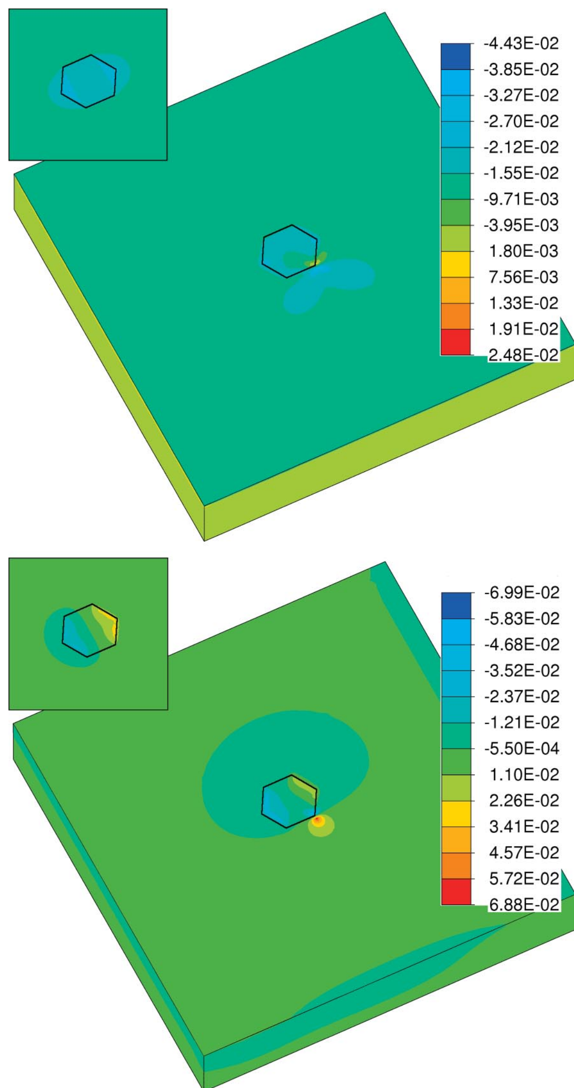

Figure 2 Surface plot through the base of the QD showing the elastic strain in the presence of a TD (*cf.* Fig. 1). Upper panel:, xx-component of strain for a ED; and lower panel, xz-component of strain for a SD. The inset of each figure shows the same strain component in the Reference configuration.

ted as a line through the centre of the quantum dot that does not pass directly through the dislocation centre; see Fig. 1. In the Reference configuration, in agreement with previous simulations [13], is symmetric in the x direction and represents a dipole in the z-direction with the negative pole at the QD base and the positive pole at the QD hat. The presence of a charged dislocation on the edge of the QD causes a linear shift of the built-in electrostatic potential along z-direction (Fig. 3b) and a *nonlinear* shift of the built-in electrostatic potential in the in-plane direction (Fig. 3a). The explanation for this, is that the potential distribution related to the dislocation decreases exponentially in the xy-plane as a function of distance from the dislocation core [4], whereas in the z-direction, the potential is a (negative) constant. The result is the formation of an asymmetric double-well potential in $-V(x)$ with the shallower well located closer to the dislocation centre. This is particularly fortuitous in the case of the SD, which has a higher charge density at the core ($1.0\,{}^{e}/_{c}$). In that specific case the potential barrier height is $271/123$ mV measured from the upper/lower wells respectively. Similarly, in the presence of an ED, formation of an asymmetric double-well potential is also observed (with barrier heights $185/141$ mV). The barrier asymmetry, *ie.* the energetic difference between the potential well and the barrier height, is: 0 mV (Ref.), 44 mV (ED), and 148 mV (SD), and can be loosely interpreted as a scheme in which excess electrons present in the QD system can tunnel away from the dislocation centre. The asymmetry is much larger for the QD-plus-SD system since the charge density is higher and decays less rapidly than for the charge density of the ED; thus its affect on the built-in potential is stronger. This notable behaviour arises because, as sketched in Section 2, the peak potential at the SD core (-1.4 V) is comparable to the built-in potential of the Reference QD (±1.35 V).

Table 1 Values of the band gap energy $E_{\mathrm{gap}}(z)$ in units of eV, calculated along the z-axis, *cf.* Fig. 3d.

	Bulk	Ref.	ED	SD
$\min[E_{\mathrm{e}}]$	3.510	2.189	2.314	2.631
$\max[E_{\mathrm{h}}]$	0.000	1.019	1.165	1.493
E_{gap}	3.510	1.170	1.149	1.138

Another test for the affect of a nearby TD on a QD is to examine the electron-hole band energies, given graphically in the lower panel of Fig. 3 with the peak band energies annotated in Tab. 1. The *classical* band gap energy E_{gap} is estimated by the difference between the electron E_{e} and hole E_{h} band energies,[1] while the electron/hole band energy is determined by subtracting electrostatic potential given in Fig. 3a-b from the bulk crystal band parameter. It is observed that the presence of a charged threading dislocation induces an approximately linear negative shift in the band energies; see Fig. 3c-d. The results presented in Tab. 1 show a systematic change in the effective band gap energy, calculated in the center of QD, with a reduction of $\sim$1.8 % (ED) and $\sim$2.7 % (SD) with respect to the band gap energy of the Reference configuration. This is a relatively small change, though together with shift of carriers localisation observed on Fig. 3c may have a measurable affect on the optical spectrum of such QDs.

4 Summary The elastic and electric fields surrounding a QD that is nucleated on the edge of a charged TD

[1] It is emphasised that a classical band gap energy is considered here and that the energy difference after quantisation is slightly larger as a consequence of Heisenberg's uncertainty principle.

© 2012 WILEY-VCH Verlag GmbH & Co. KGaA, Weinheim

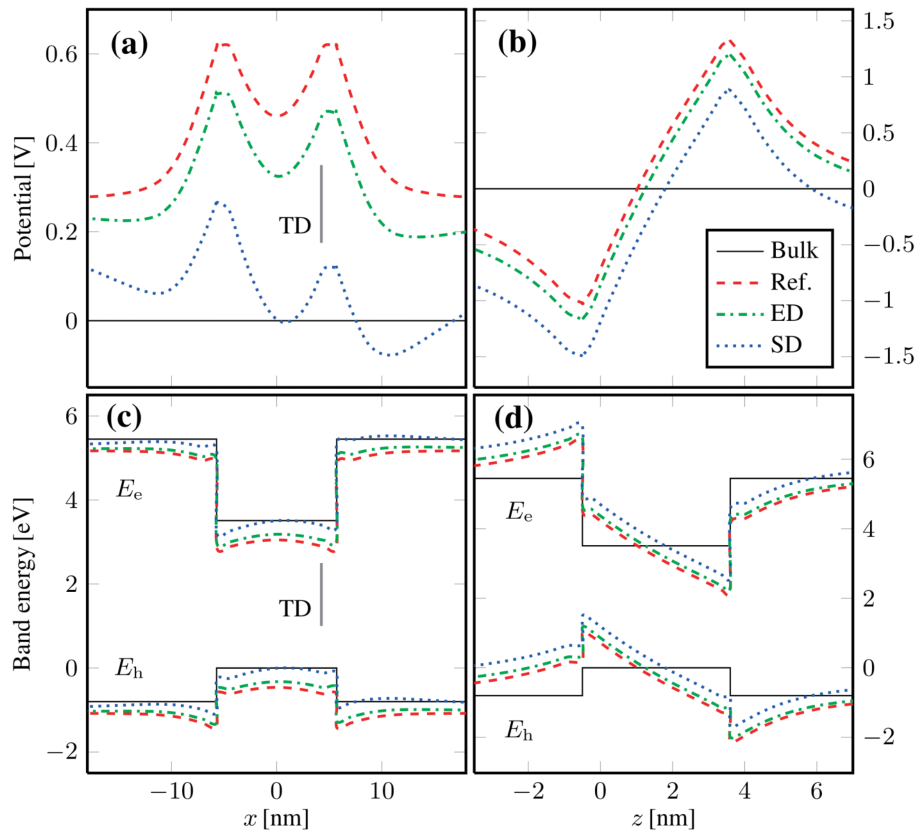

Figure 3 Line plots of the electrostatic potential (upper panel) and band energies (lower panel) through the centre of the QD in the x-direction and the z-direction in the presence of a TD (marked by a short vertical line). Reference configuration (Ref.) and bulk material quantities are included. Note: Owing to the approximately spherical symmetry of the QD in the xy-plane, the quantities displayed and measured in the y-direction (not shown) are strikingly similar to those in the x-direction (see the main text).

were modelled. The effects of an ED and a SD were compared with a Reference configuration (absence of a TD). The explanation that a TD provides a region for preferential QD nucleation by inducing partial strain relief on the QD, was supported here by the appearance of a region local tensile strain (rather than compressive strain) on the QD corner close to the dislocation line. Since the Burgers vector of the SD is coaxial with the dislocation line, effects mainly arise in the shearing components of strain in planes parallel to the dislocation line. The overall result obtained from the strain change and charged dislocation line is a negative shift of the built-in QD potential and the formation of an asymmetric double-well potential in $-V(x)$ with the shallower well located closer to the dislocation centre. A measurable reduction in the effective band gap energy follows, nevertheless, this change is rather subtle due to the large band gap nature of bulk GaN and AlN. It remains an open question as to the magnitude of the affect this would have on the localisation of electron/hole wavefunctions. This is to be the focus of future work.

Acknowledgements This work was supported by the Polish Ministry of Science and Higher Education under grant numbers N519 402837 and N519 647640.

References

[1] S. C. Jain, M. Willander, J. Narayan, and R. V. Overstraeten, J. Appl. Phys. **87**, 965 (2000).
[2] L. Jiawei, Y. Zhizhen, and N. M. Nasser, Physica E **16**, 244–252 (2003).
[3] P. J. L. Rouviere, J. Simon, N. Pelekanos, B. Daudin, and G. Feuillet, Appl. Phys. Lett. **75**, 2632 (1999).
[4] J. Cai and F. A. Ponce, Phys. Status Solidi A **192**(2), 407–411 (2002).
[5] D. Cherns and C. G. Jiao, Phys. Rev. Lett. **87**(20), 205504(4) (2001).
[6] A. D. Andreev, J. R. Downes, and E. P. OReilly, Physica E **13**, 1094 1097 (2002).
[7] P. Dłużewski, T. D. Young, G. Jurczak, and J. A. Majewski, Phys. Status Solidi C **4**(7), 2399 (2007).
[8] J. F. Nye, Physical Properties of Crystals: Their Representation by Tensors and Matrices (Clarendon Press, Oxford, 1957).
[9] P. Dłużewski, G. Maciejewski, G. Jurczak, S. Kret, and J. Y. Laval, Comput. Mater. Sci. **29**, 379 (2004).
[10] A. E. H. Love, Mathematical Theory of Elasticity (Cambridge University Press, Cambridge, 1927).
[11] P. Dłużewski, T. D. Young, G. Dimitrakopulos, and P. Komninou, IJMCE **8**(3), 331–342 (2010).
[12] I. Vurgaftman and J. R. Meyer, J. Appl. Phys. **94**(6), 3675(22) (2003).
[13] G. Jurczak and T. D. Young, Appl. Surf. Sci. (2012), in press. http://dx.doi.org/10.1016/j.apsusc.2012.04.005.

© 2012 WILEY-VCH Verlag GmbH & Co. KGaA, Weinheim